Applied Microbiology and Biotechnology (2024) 108:84
https://doi.org/10.1007/s00253-023-12867-9

BIOTECHNOLOGICALLY RELEVANT ENZYMES AND PROTEINS

Biosynthesis of eriodictyol in citrus waster by endowing P450BM3 activity of naringenin hydroxylation

Xingyi Zhang[1] · Yinghui Feng[2] · Yuanzhe Hua[1] · Chuanxi Zhang[3] · Bohuan Fang[3] · Xiang Long[1] · Yue Pan[2] · Bei Gao[4] · John Z. H. Zhang[2,5] · Lijun Li[1] · Hui Ni[1] · Lujia Zhang[2,5]

Received: 20 June 2023 / Revised: 20 September 2023 / Accepted: 13 October 2023

Abstract

The flavonoid naringenin is abundantly present in pomelo peels, and the unprocessed naringenin in wastes is not friendly for the environment once discarded directly. Fortunately, the hydroxylated product of eriodictyol from naringenin exhibits remarkable antioxidant and anticancer properties. The P450s was suggested promising for the bioconversion of the flavonoids, but less naturally existed P450s show hydroxylation activity to C3′ of the naringenin. By well analyzing the catalytic mechanism and the conformations of the naringenin in P450, we proposed that the intermediate Cmpd I ((porphyrin) Fe = O) is more reasonable as key conformation for the hydrolyzation, and the distance between C3′/C5′ of naringenin to the O atom of CmpdI determines the hydroxylating activity for the naringenin. Thus, the "flying kite model" that gradually drags the C-H bond of the substrate to the O atom of CmpdI was put forward for rational design. With ab initio design, we successfully endowed the self-sufficient P450-BM3 hydroxylic activity to naringenin and obtained mutant M5-5, with k_{cat}, K_m, and k_{cat}/K_m values of 230.45 min^{-1}, 310.48 μM, and 0.742 min^{-1} μM^{-1}, respectively. Furthermore, the mutant M4186 was screened with k_{cat}/K_m of 4.28-fold highly improved than the reported M13. The M4186 also exhibited 62.57% yield of eriodictyol, more suitable for the industrial application. This study provided a theoretical guide for the rational design of P450s to the nonnative compounds.

Key points

- *The compound I is proposed as the starting point for the rational design of the P450BM3*
- *"Flying kite model" is proposed based on the distance between O of Cmpd I and C3′/C5′ of naringenin*
- *Mutant M15-5 with 1.6-fold of activity than M13 was obtained by ab initio modification*

Keywords Naringenin · Eriodictyol · P450BM3 · Flying kite model

Introduction

The reprocessing of agricultural waste has always been a significant concern, as it could improve the product additional value and protect the environment (Khan et al. 2021;

Xingyi Zhang and Yinghui Feng contributed equally to this work.

✉ Hui Ni
nihui@jmu.edu.cn

✉ Lujia Zhang
Ljzhang@chem.ecnu.edu.cn

[1] College of Ocean Food and Biological Engineering, Jimei University, Xiamen 361021, China

[2] Shanghai Engineering Research Center of Molecular Therapeutics & New Drug Development, School of Chemistry and Molecular Engineering, East China Normal University, Shanghai 200062, China

[3] Department of Micro/Nano Electronics, School of Electronic Information and Electrical Engineering, Shanghai Jiao Tong University, Shanghai 200240, China

[4] School of Health Science and Engineering, University of Shanghai for Science and Technology, Shanghai 200093, China

[5] NYU-ECNU Center for Computational Chemistry at NYU Shanghai, Shanghai 200062, China

Published online: 08 January 2024

Sharma and Lee 2017). However, the compounds of steroids (Acevedo-Rocha et al. 2018; Kille and Reetz 2011; Li and Reetz 2020), alkanes (Chen and Cong 2019; Karasawa and Watanabe 2018), and flavonoids (Chu and Sohng 2016; Hong and Kong 2020; Nguyen and Yun 2020a, b, 2021) that widely exist in agricultural waste are hard to be converted into high-valued pharmaceutical molecules. Naringenin is a kind of flavonoid in citrus waste (Sharma and Lee 2017), and its hydroxylated product eriodictyol was an effective medicine with properties of anti-cancer (Chu and Sohng 2016), anti-inflammatory(Lee and Kim 2013), anti-apoptotic, and antioxidant (Lee and Cho 2007). The eriodictyol was also widely used as precursor in the synthesis of taxifolin, proanthocyanidins, anthocyanins (Owens and Winkel 2008), and silibinin (Lv and Zhou 2019). In 1999, Kaltenbach and Schröder (1999) achieved eriodictyol biosynthesis by co-expression of flavonoid hydroxylase P450 (F3′H) and P450 reductase from *Catharanthus roseus* in *Escherichia coli*. However, both the expression and selective activity of the recombinant protein were poor. In 2010, Amor and Ghoul (2010) obtained a high yield of 200 mg/L for eriodictyol by expressing bioflavonoid 3′hydroxylase (F3′H) from gerberas, but the activity of these plant-derived F3′H/CPRs was decreased significantly once being expressed in yeast. Despite the several achievements in eriodictyol synthesis with different P450s (Amor and Ghoul 2010; Kaltenbach and Schröder 1999; Kasai and Sakaki 2009), challenges like low expression and insufficient activity remain.

P450BM3 (CYP102A1), derived from *Bacillus macros*, possesses advantages of self-sufficiency, highly solubility, high hydroxylation activity, and broad substrate spectrum (Whitehouse and Wong 2012). Also, the P450BM3 and its mutants have great potential towards in hydroxylating steroids (Acevedo-Rocha et al. 2018; Kille and Reetz 2011; Li and Reetz 2020), alkanes (Chen and Cong 2019; Karasawa and Watanabe 2018), flavonoids, and their derivatives (Chu and Sohng 2016; Hong and Kong 2020; Nguyen and Yun 2020a, b, 2021). Kille and Reetz (2011) and Li and Reetz (2020) and Chen and Wong (2020) have achieved specifically stereoselective hydroxylation of steroids like testosterone, androstenedione (AD), dehydroepiandrosterone (DHEA), and testosterone (TST) via P450BM3 modification. In 2016, Chu and Sohng (2016) obtained two mutants of M13 and M15 by modifying the inactive P450BM3 and successfully converted naringin into eriodictyol, providing a new clue for eriodictyol biosynthesis. However, the activities of M13 and M15 are very low. Detailed structural analysis and better design strategy for the rational design are necessarily needed to obtain mutants with high activity. Due to the indeterminacy of the core catalytic model, rational design efforts for eriodictyol in P450BM3 are unproductive, less mutants with highly active reported thus far. The catalytic mechanism of P450 has been demonstrated to involve a nine-step cycle; however, consensus on which step is more reasonable for rational design has not yet reached. Given the consistent presence of iron-porphyrin in reported P450 structures, it has commonly served as the starting point for molecular modifications. Sun and Li (2020) and Hong and Kong (2020) utilized iron-porphyrin as the starting point and successfully developed mutants with high hydroxylation activity to steroids. However, the intermediates of porphyrin-Fe^{III}-OOH (Cmpd 0), porphyrin-Fe^{IV}=O (Cmpd I), and porphyrin-Fe^{IV}-OH (Cmpd II) were highly involved the catalyzation, compared to iron-porphyrin. Moreover, the formation of compound I (Cmpd I, porphyrin (Fe=O) was considered the limit step in the hydroxylation (Huang and Groves 2017; Sligar 2010). Thus, the starting structure for the rational design needs further analysis.

In this paper, the Cmpd I is proposed more reasonable as the starting structure than Fe-porphyrin for the rational design of P450BM3. Additionally, a "flying kite model" is put forward based on the distance between the oxygen atom of Cmpd I and the hydroxylated site C3′/C5′ of naringenin. By gradually dragging naringenin closer to the oxygen atom of Cmpd I, two mutants, M4186 and M5-5, were respectively obtained. This ab initio design approach for P450BM3 offers valuable guides for endowing enzymes activity towards novel substrates, thereby expanding their potential applications in industry and pharmacy.

Material and methods

Plasmids, microorganisms, and media

The P450BM3 gene (NCBI: CP001982.1) was cloned in the plasmid pET28a. The constructed plasmid P450BM3-pET-28a was used as template to construct mutants M13, M4186, and M5-5 using a point mutation system with the primers in Table S2. Mutagenesis was performed using the Blunting Kination kit. Subsequently, the modified plasmids were transformed and replicated into competent *E.coli* DH5α cells. Competent *E.coli* BL21 (DE3) cells were used as expression hosts and transferred using the heat shock method (Liu et al. 2021). Colony PCR was employed for the validation of successful transformation, while DNA sequencing was utilized for the identification of mutants.

Protein expression and purification of mutants

The colonies were picked and grown in 5 mL of Luria–Bertani medium containing kanamycin (50 μg/mL), and incubated overnight in a shaker at 37 °C and 220 rpm. The cultured cells were then inoculated in 500 mL of LB medium with kanamycin (50 μg/mL) at a 1% v/v ratio. Isopropyl-β-d-thiolaldehyde glycoside (0.5 mM) and 5-aminolevulinate

hydrochloride (1.0 mM) were added to the medium for enzyme induction when the OD_{600} reached between 0.6 and 0.8. The cells were incubated for 12 h at 20 °C/220 rpm and harvested via centrifugation for 5 min at 8000 rpm and 4 °C. The cells were resuspended in buffer A (50 mM Tris–HCl, 100 mM NaCl, 10% glycerol, pH 7.4) and washed three times. Afterwards, the cells were resuspended in Buffer A at a ratio of 1 g cells/7 mL and sonicated for 40 min in an ice bath using a 5 s:5 s sonication:pause interval. The cell fragments were centrifuged at 18,000 g for 20 min at 4 ℃, and the supernatant was filtered through a 0.22-μm Millipore filter. The obtained supernatant was purified using Ni affinity chromatography and validated with SDS-PAGE (Fig. S1). Protein concentrations were quantified via Bradford method with bovine serum albumin as the standard.

Enzymatic activity assay and kinetic measurements

The 500-μL volume of reaction is catalyzed in potassium phosphate buffer (100 mM, 10% glycerol, pH 7.4). The composition of the reaction was as follows: 1 μM purified P450 BM3, 0.1 mM naringenin, 5 mM glucose, 1 mM $NADP^+$ and GDH crude enzyme. After incubating for 2 h at 37 °C, the reaction was terminated by adding 1 mL methanol and was shake for another 10 min. The terminated reaction solution was centrifuged at a speed of 20,000 g for 20 min. The supernatant was collected and subjected to high performance liquid chromatography-photodiode array (HPLC–PDA) for further analysis. The kinetic parameters of the mutants were determined by quantifying different concentrations of naringenin. The experimental data were fitted to the Michaelis-Menten kinetic model to obtain the kinetic parameters (Nguyen et al. 2021; Nguyen and Yun 2021).

Whole cell biotransformation of naringenin

The colony was cultured in 5 mL of LB medium containing kanamycin (50 μg/mL), and were then incubated in a shaker at 37 °C and 220 rpm for roughly 8 h. Subsequently, 200 μL of the inoculate was transferred to a 250-mL flask containing 50 mL of 1 × M9 medium with kanamycin (50 μg/m). Once the OD_{600} reached 0.8–1.0, 0.5 mM IPTG and 1 mM 5-aminolevulinic acid were added to induce the protein expression. The cells were incubated at 22 °C and 200 rpm for another 12 h. Naringenin dissolved in dimethyl sulfoxide (DMSO) was added to the culture at a final concentration of 100 μM and further incubated at 28 °C. Samples were collected periodically using aliquots of 1 mL, which were subsequently subjected to centrifugation and freeze-drying processes. The resulting freeze-dried samples were reconstituted using methanol (1 mL), followed by centrifugation at 20,000 g for 20 min prior to analysis via HPLC–PDA.

Molecular docking and MD simulations

The heme domain of P450BM3 (PDB: 1BU7) was downloaded from the database https://www.rcsb.org/ and imported into the Maestro program after removing water molecules. The iron porphyrin was isolated, and an oxygen atom was added to the Fe^{2+} of the iron porphyrin using the Draw option, with a set Fe = O bond length of 1.65 Å. This constructed Cmpd I was then used to replace the iron porphyrin in 1BU7 using the Discovery Studio 2019 software for subsequent simulation and design. The complexed structure of the heme domain with Cmpd I underwent minimization before molecular docking of naringenin using Maestro program. The overall geometry optimization was performed with OPLS3e, setting the O atom of Cmpd I as the docking center within a box size of 20Å × 20Å × 20Å. The ligand of naringenin was first prepared at pH 7.0 ± 2.0 using LigPrep and was then docked into active site of the built structure using the program of Docking module with standard precision (SP). The top ten conformations were collected and all structures were visually analyzed using the DS program.

Results

The catalytic core model for the near-attack state

The key factor in converting naringenin into eriodictyol for P450BM3 is to place the nonnatural ligand at a specific conformation with an optimal catalytic distance (Fig. 1A). However, there is still challenge how to precisely define this catalytic distance. Extensive studies have elucidated that the hydroxylation mechanism of P450BM3 involves nine steps, with multiple reduction and oxidation reactions (Fig. 1B). However, it is still not determined whether the popherin-Fe^{2+} or Cmpd I is more reasonable as the starting point for P450-BM3 modification. At present, most P450 modification was conducted by (1) blind direct/saturation mutagenesis and (2) substrate conformation-focused mutagenesis, with ferroporphyrin as the starting structure. Herein, we attention to the bio-catalyzation (proton/electron transfer) to determine the starting structure and define the catalytic distance. In P450BM3, snatching the H· from the substrate by Cpmd I (step7, Fig. 1B) was the step directly involved in the hydroxylation and eriodictyol synthesis. Thus, the Cmpd I was proposed more reasonable as the starting point for the rational design compared to the other intermediates of iron porphyrin, ferroporphyrin-OOH, or iron porphyrin-OO^- synthesized in the catalytic cycle (Jiang and Li 2021; Ogliaro and Shaik 2002; Su and Shaik 2019; Wang and Shaik 2015). The distance between the O atom of Cmpd I and the C3′ atom of the naringenin determines the catalytic activity and stereo-selectivity. In 2010, Rittle and

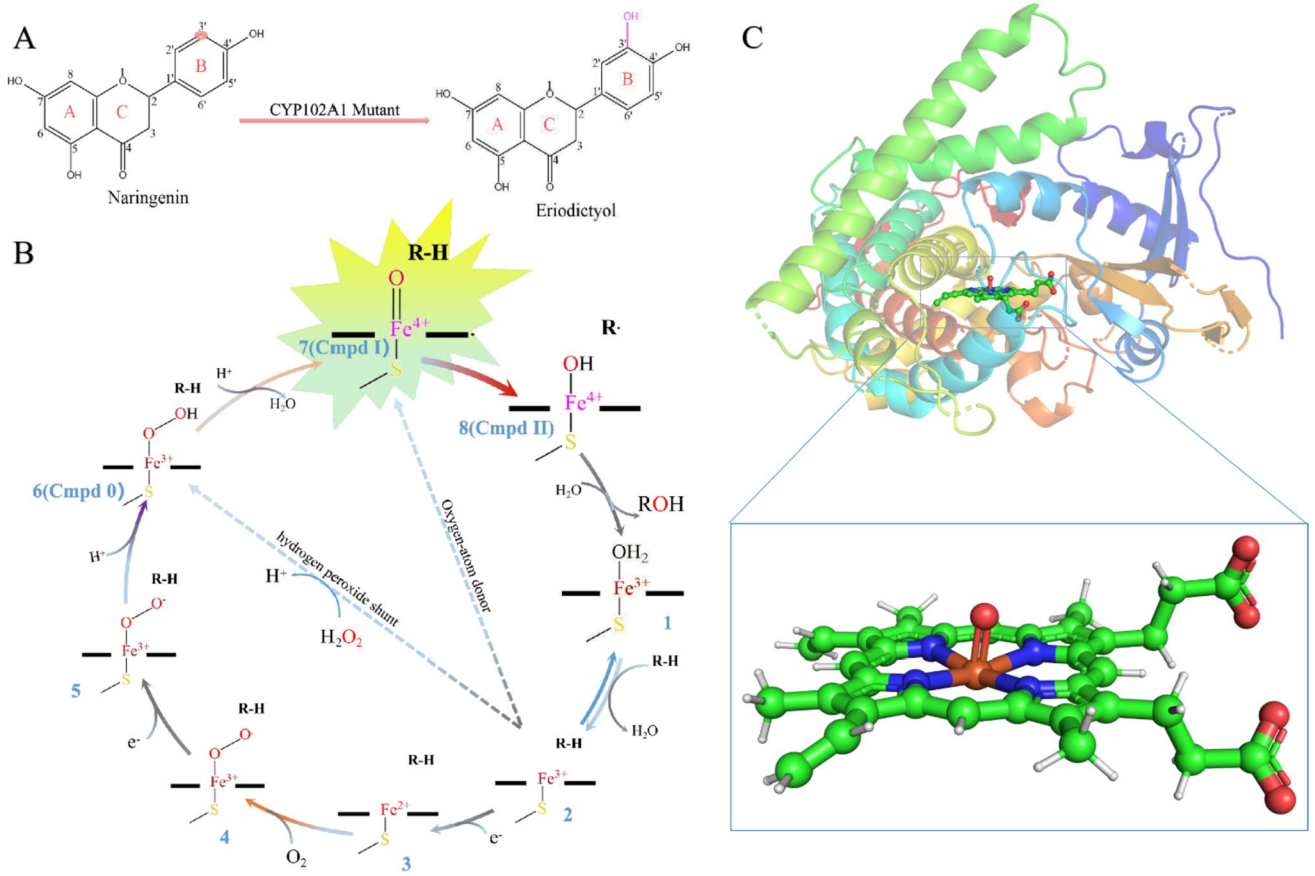

Fig. 1 **A** P450 BM3 mutants catalyzed regioselective hydroxylation of naringenin to produce eriodictyol. **B** The catalytic mechanism cycle for the hydroxylation of P450. **C** Catalytic intermediate (Cmpd I) model for the rational design put forward in this paper

Green Michael (2010) captured the P450 (CYP119)-Cmpd I complex and determined the Fe = O bond to be 1.68Å by low temperature crystallization. Therefore, we were able to obtain the structure of Cmpd I in the heme domain (PDB ID: 1BU7) by constructing Fe = O bonds on porphyrin-Fe (Fig. 1C), and analyzed the relationship and influence of the distance between the O atom of Cmpd I and the C3′/C5′ atom of the substrate B ring on the catalytic activity and selectivity.

We identified the influence factors of hydroxylation activity, through the analysis of naringenin in WT, M13 (R47L/L86I/F87V/L188Q), and M15 (R47L/E64G/F87V/E143G/L188Q/E267V) active center of conformational change. As shown in Fig. 2I, the A ring of naringenin in WT is close to the Cmpd I, causing the hydroxylation site C3′ on the B ring extremely far away from the active O atom (13.9 Å). In contrast, the R47L, F87V, and L188Q mutations in M13 and M15 provided additional substrate space and allowed naringenin to flip 180°, causing the B ring stretching deep into the catalytic site. The farther distance caused by the incorrect conformation in the active site of the wide P450BM3 is believed to be the main barrier for its catalytic activity to naringenin. It is of note that the naringenin in both M13 and M15 was stretched in two conformations at the B ring, both parallel and perpendicular to the porphyrin. The distance between the C3′ of both the parallel and vertical naringenin and the O atom of Cmpd I in M15 was 4.51 and 4.28 Å, respectively (Fig. 2II; Fig. S2), whereas those in M13 were 4.06 and 3.85 Å (Fig. 2III). The closer catalytic distance of M13 than M15 suggested a better hydroxylation activity, which was consistent with the experimental observations: M13 showed higher naringenin-hydroxylating activity than M15 (Chu and Sohng 2016).

With precondition of correct stretching manners of the naringenin in the active site, shorter distances between the catalytic atoms of the ligand and Compound I could highly improve the hydroxylation activity. Therefore, in rational design, we treated the substrate as a kite and tried to improve the catalytic activity by constantly dragging the C3′/C5′ of naringenin closer to the Compound I O atom of Cmpd I. In each round of screening, the mutant with the nearest catalytic distance and minimum binding energy was picked for experimental verification. We call this design strategy as "flying kite model" (Fig. 3A).

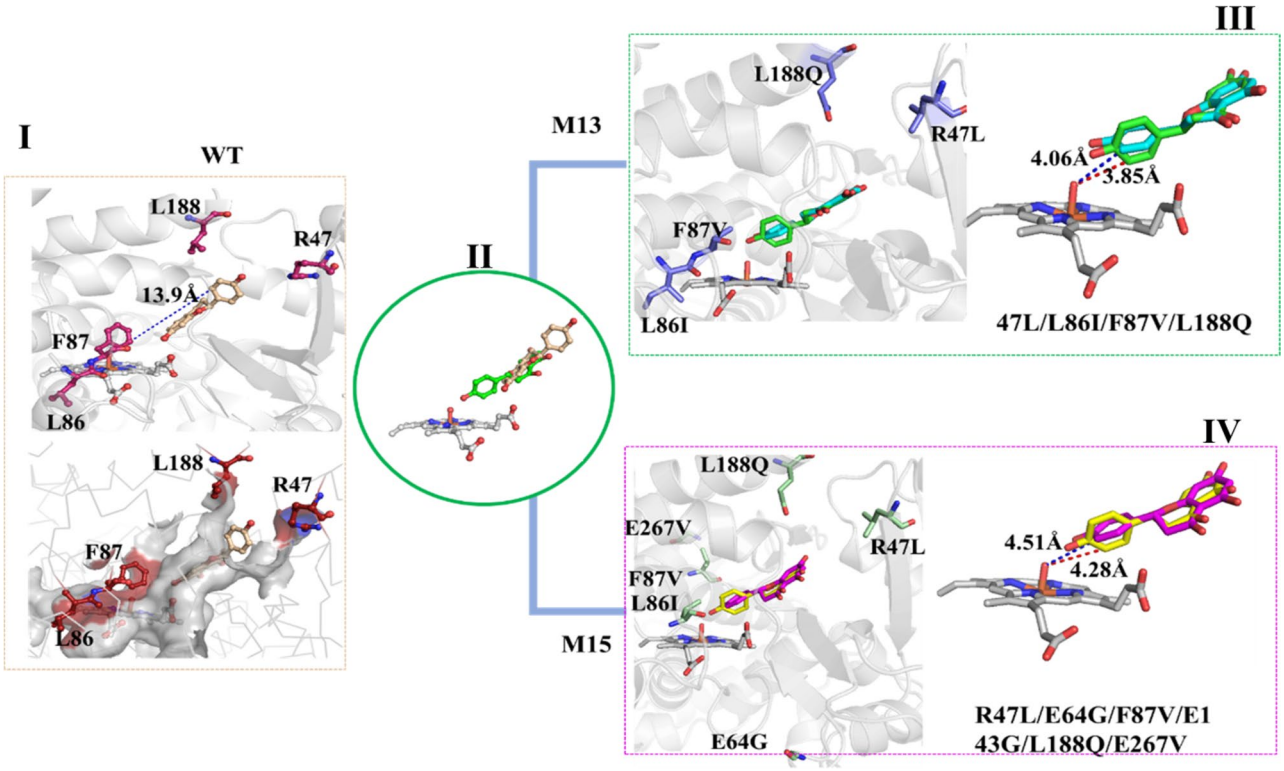

Fig. 2 Binding state of the substrates in the P450 BM3(I), M13 (II), and M15 (III). I, the ligand naringenin flipped away in the active pocket of wide type P450BM3, and the distance of catalytic site C3′ of and the O atom of the Cmpd I is 13.9 Å. II and III, the ligand in M13 and M15 stretched correctly with the B ring close to Cmpd I. There were parallel and vertical conformations of naringenin in M13 (green and cyan sticks) and M15 (magenta and yellow sticks), and the corresponding distances were respectively 4.06/3.85 Å and 4.51/4.28 Å. The residues in the WT, M13, and M15 were respectively shown as red, slate and lemon sticks. And the CmpdI was shown as grey sticks

Modification of M13 using the "flying kite model"

Based on the above "flying kite model," we utilized M13 with the highest activity as the starting point for mutation design. We selected residues within 20 Å range in the active pocket (Fig. 3B; Table S3), which are known to be involved in flavonoid catalysis (Table S1), for mutagenesis. Thirteen of these residues were used for mutation design, and naringenin had vertical and parallel conformations in these mutants. However, except for mutant M4186, all mutants exhibited longer distances between their catalytic atoms (C3′ of naringenin and O of Cmpd I) compared to M13's distance of 3.82 Å. The catalytic distances in mutant M4186 were measured at 4.13 and 3.80 Å, respectively (Fig. 3C and D). The construction of M4186 was therefore picked for experimental verification. The total turnover number (TTN, nmol product/nmol enzyme) of M4186 is 86.4, 2.32 times higher than that of M13 (37.2) (Fig. 5A and B). The dynamic parameters of K_m and k_{cat} to the naringenin were respectively 182.339 ± 23.369 μM and 389.79 ± 15.4 min^{-1}, also suggesting a better improvement of ligand specificity and catalytic effectivity than the wide type M13 (479.745 ± 103.448 μM and 215.83 ± 21.04 min^{-1}, respectively) (Table 1).

Ab initio design of P450BM3 with "flying kite model"

As the "kite model" was putted forward based on the key catalytic step of P450BM3, we propose that this model is not only applicable to M13 but also suitable for designing P450BM3 from scratch. Thus, several rounds of rational designs to the wide type P450BM3 were performed (Table S4).

Dragging the substrate into the binding pocket and maintaining the correct conformation are key steps for P450BM3 to catalyze naringenin (Fig. 2). As shown in Fig. 4 ①, in the first round of mutations, the F87V mutant successfully motivated this flipping motion, making the distance between C3'/C5' and the catalytic center Fe = O the shortest (4.16–4.22 Å). The high docking score (> − 6 kcal/mol), closer distance, and reasonable conformation led us to choose F87V as the template for the second round of mutations. The lower catalytic distance (lower

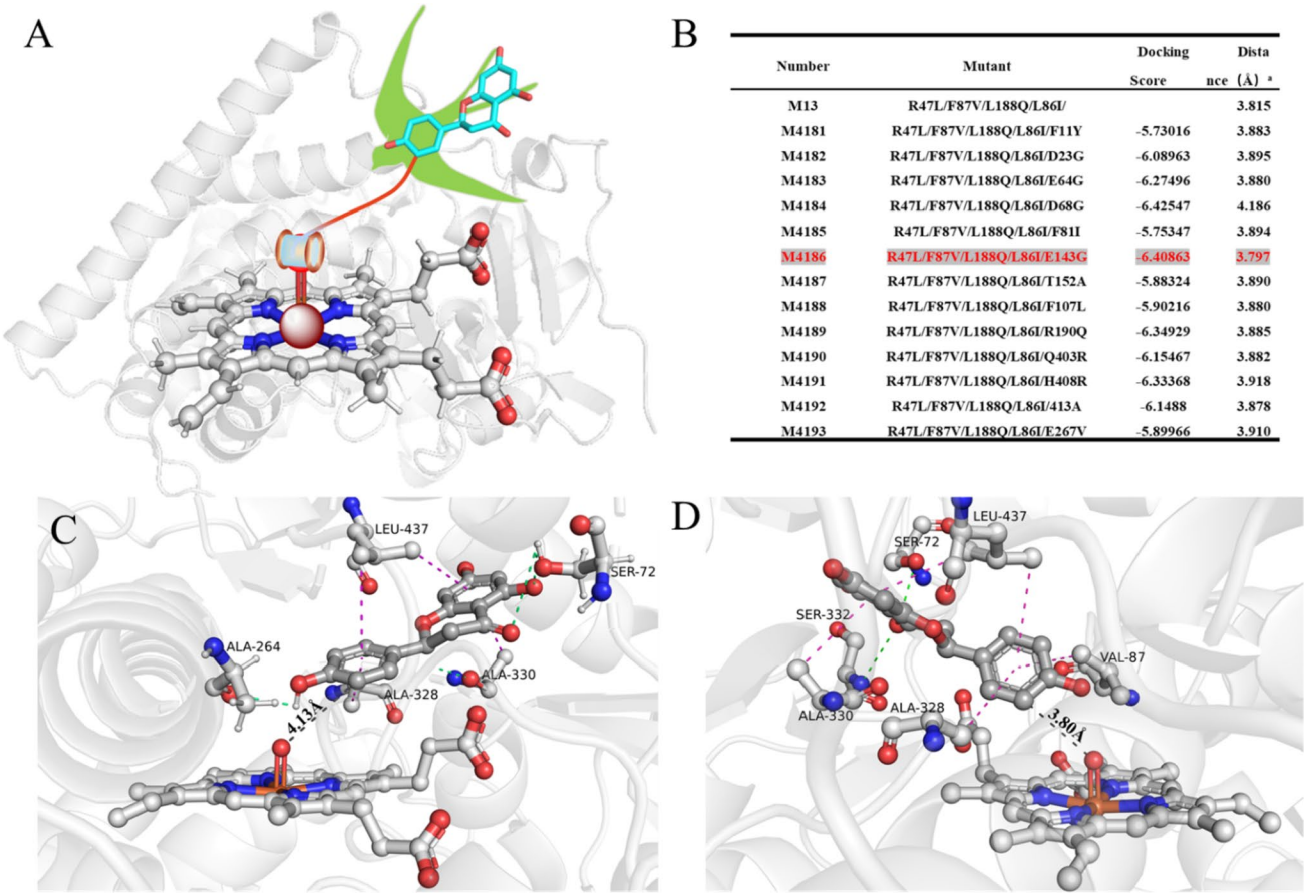

Number	Mutant	Docking Score	Distance (Å) [a]
M13	R47L/F87V/L188Q/L86I/		3.815
M4181	R47L/F87V/L188Q/L86I/F11Y	-5.73016	3.883
M4182	R47L/F87V/L188Q/L86I/D23G	-6.08963	3.895
M4183	R47L/F87V/L188Q/L86I/E64G	-6.27496	3.880
M4184	R47L/F87V/L188Q/L86I/D68G	-6.42547	4.186
M4185	R47L/F87V/L188Q/L86I/F81I	-5.75347	3.894
M4186	R47L/F87V/L188Q/L86I/E143G	-6.40863	3.797
M4187	R47L/F87V/L188Q/L86I/T152A	-5.88324	3.890
M4188	R47L/F87V/L188Q/L86I/F107L	-5.90216	3.880
M4189	R47L/F87V/L188Q/L86I/R190Q	-6.34929	3.885
M4190	R47L/F87V/L188Q/L86I/Q403R	-6.15467	3.882
M4191	R47L/F87V/L188Q/L86I/H408R	-6.33368	3.918
M4192	R47L/F87V/L188Q/L86I/413A	-6.1488	3.878
M4193	R47L/F87V/L188Q/L86I/E267V	-5.89966	3.910

Fig. 3 **A** The "flying kite model" put forward for the rational design. The distance between the 3′ and 5′ carbon to the O of the compound I was the key values for the mutagenesis. **B** The docking score and distances of the mutants, and the mutant M4186 was the best one for the catalyzation. **C** and **D** The binding manners of the parallel and vertical conformation of the substrate naringenin at the active site of M4186. The corresponding residues were shown in sticks, and the van der Waals forces were shown in dashed red and green lines

Table 1 Kinetic parameters of P450BM3 mutants for the hydroxylation of naringenin

Mutant	k_{cat} (min^{-1})	K_m (μM)	k_{cat}/K_m (min^{-1} μM^{-1})
WT[a]	ND	ND	ND
M13	215.83 ± 21.04	479.745 ± 103.448	0.500
M4186	389.79 ± 15.4	182.339 ± 23.369	2.138
M5-5	230.45 ± 20.32	310.48 ± 72.22	0.742

[a]Incompetence

than 4.9 Å) and docking fraction (− 5.5 ~ − 6 kcal/mol) in the second round of mutations suggest that it was right to choose F87V as the template. Among all the double mutants, F87V/L188Q performed the best. The distance between Cmpd I and the substrate was 4.13–4.18 Å (Fig. 4 ②), while the distance between C5′ and reactive oxygen atoms was only 4.13 Å. Consequently, F87V/L188Q was chosen as a template for subsequent design iterations. In the third and fourth rounds of mutagenesis, F87V/L188Q/R47L and F87V/L188Q/R47L/E143G were obtained as optimal mutants based on their lower catalytic distances and docking scores (Fig. 4 ③ and ④). However, these mutants selected in the first four rounds shown no hydroxylation activity once constructed in *E. coli* BL21 (DE3), suggesting that these mutagenic efforts were still insufficient to achieve effective hydroxylation. Although there was a slight decrease in the distances between C5′/C3′ of the substrate and the O of Cmpd I (4.09–4.12 Å and 4.08–3.97 Å, respectively), as well as four and six close conformations identified in the docking simulation, more significant mutations are required to further shorten catalytic distances to catalyze the naringenin. In the fifth round of mutation, the catalytic distances of M5-5 (F87V/L188Q/R47L/E143G/H408R) were measured to be 4.06 Å (C3′) and 3.84 Å (C5′) (Fig. 4, ⑤ and II), exhibiting a great catalytic distance decrease of 0.4 Å compared to the F87V mutant (Fig. 4I). This variant was successfully expressed in *E. coli* BL21 (DE3) and displayed favorable catalytic

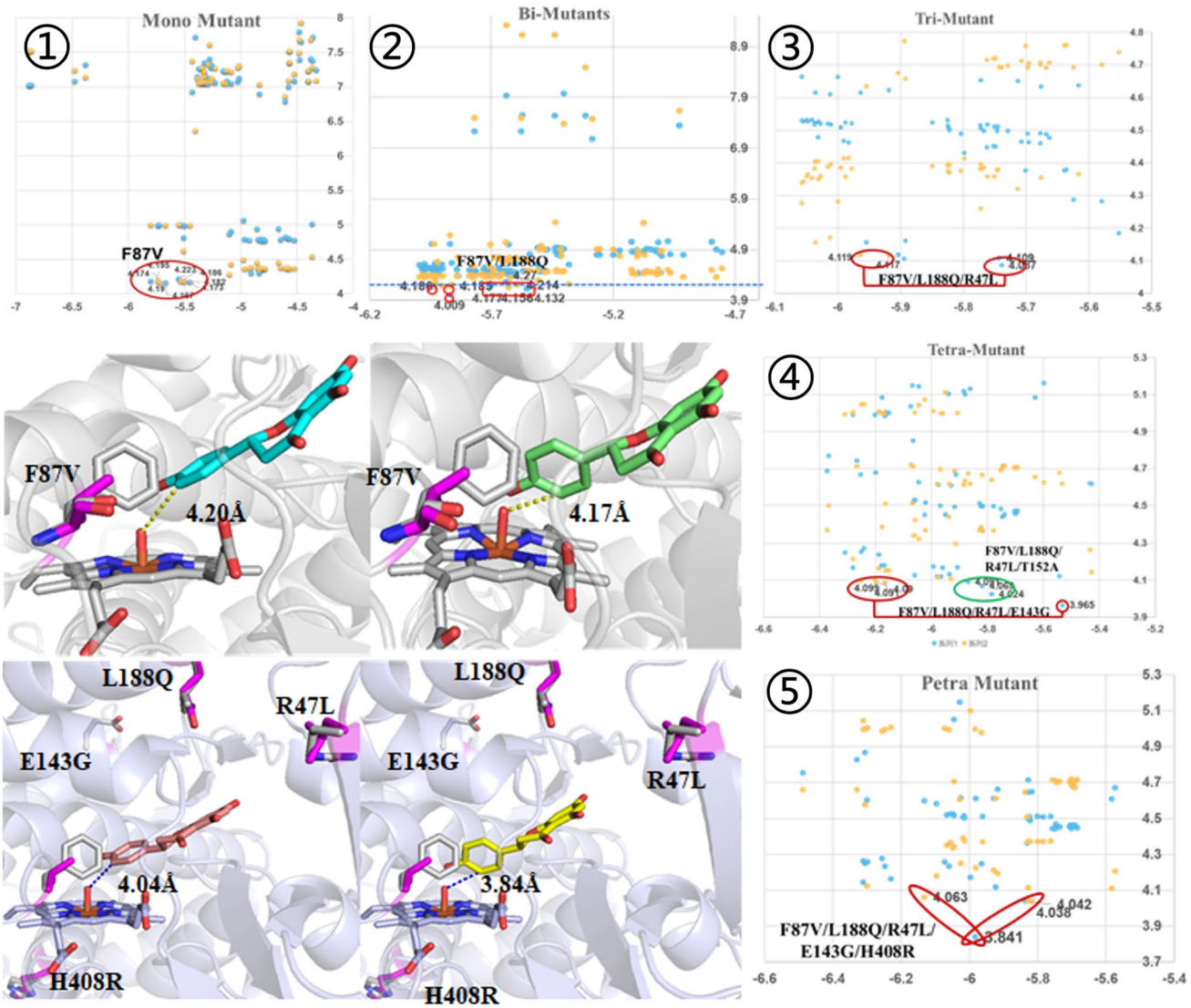

Fig. 4 Virtual mutagenesis based on the "flying kite model." ①–⑤ the docking score, distances of 3′ and 5′ carbon of the substrate with O of the compound I in different mutants. The best mutants were labeled out. I and II, the binding manners of the mono mutant F87V and the petra mutant F87V/L188Q/R47V/E143G/H408R. The initial and mutated residues were respectively show in gray and magenta sticks. The parallel and vertical stretching manners of naringenin in the two mutants were respectively shown in cyan, lime, salmon, and yellow sticks. And the distances were labeled in Å and shown in dashed yellow and blue lines

activity. The total turnover number (TTN) reached 60, which was approximately 1.6 times higher than that of M13 (Fig. 5A and B). Notably, mutant M5-5 demonstrated comparable dynamic values to M13, with k_{cat}, K_m, and k_{cat}/K_m values of 230.45 min^{-1}, 310.48 μM, and 0.742 min^{-1} $μM^{-1}$, respectively. The comparable catalytic distances of M5-5 (4.06 Å and 3.84 Å) to those of M13 (4.06 Å and 3.85 Å) (Table 1; Fig. S2) further support the notion that closer catalytic distances can enhance hydroxylation activity towards nonnatural ligands in mutants. Moreover, the reduced K_m value observed in M5-5 suggests that improved substrate recognition is a key factor contributing to enhanced hydroxylation performance.

The biosynthesis of eriodictyol with the mutants

To gain a deeper understanding of the catalytic properties of the M13, M5-5, and M4186 mutants, their catalytic behavior was comprehensively analyzed (Table 1; Figure S3). For the mutant M4186, both of the K_m, k_{cat}, and k_{cat}/K_m were highly improved than its parent M13 (with one times improved). The mutant M5-5 showed similar k_{cat} values as M13, with a better improvement in K_m (310.48 μM), suggesting that it was the higher substrate recognition manner of M5-5 that improved the hydroxylation activity. Considering the catalytic distances of M4186 (4.13 Å and 3.80 Å), M5-5 (4.06 Å and 3.84 Å), M13 (4.06 and 3.85 Å), and their dynamic

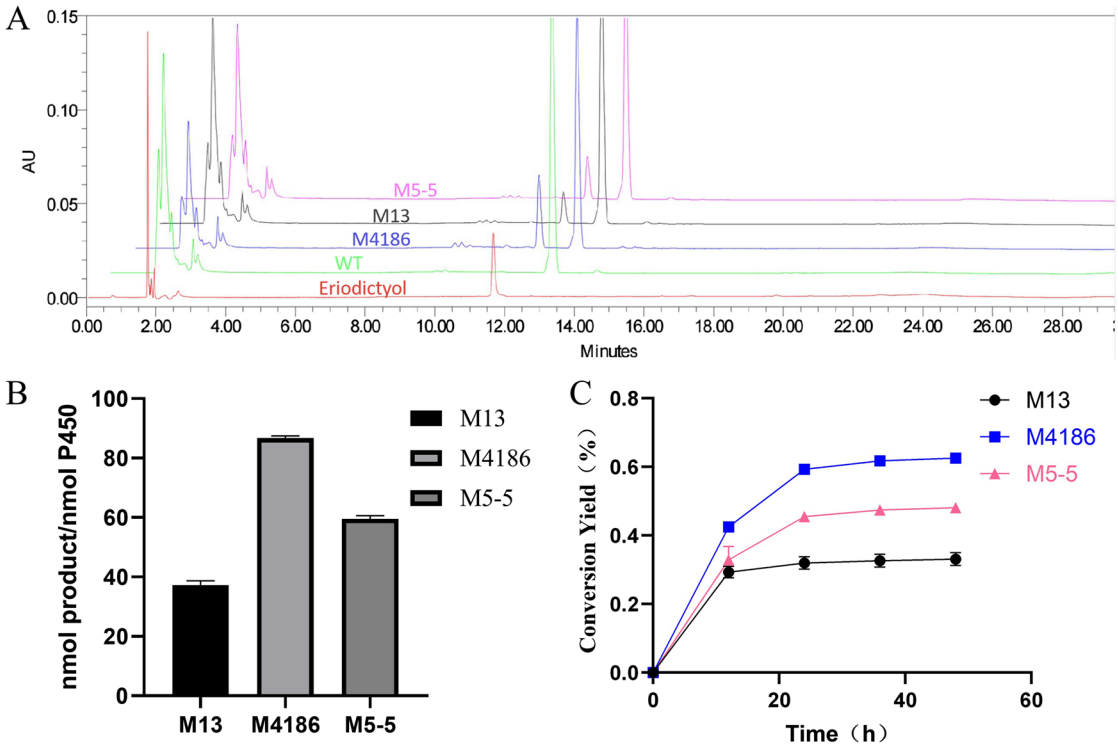

Fig. 5 **A** HPLC-PDA analysis of naringenin in vitro hydroxylation reaction mixture. **B** Total turnover numbers (TTN, nmol product/nmol enzyme) for formation of eriodictyol for the mutants. **C** Bioconversion rate of naringenin (100 μM) in 50-mL system. The data for the WT, M13, M4186, and M5-5 were respectively colored in green, black, blue and magenta

parameters, it seems that the catalytic distances lower than 3.85 Å could highly possibly endow the P450 activity to naringenin. Furthermore, once these mutants exhibit hydroxylation towards nonnatural ligands, their enhanced recognition abilities can significantly improve overall catalytic efficiency as well. To further investigate the industrial application potential of the mutants, we conducted additional studies on the bioconversion abilities of M13, M4186, and M5-5 in whole-cell catalysis models (Fig. S4). As shown in Fig. 5C, both M4186 and M5-5 exhibited efficient substrate conversion within 24 h, with conversion rates of 60.37% and 42.28%, respectively, significantly higher than that of M13 (36.25%) and almost reached equilibrium. After 48 h of whole-cell catalysis, the naringenin conversion rates catalyzed by M4186 and M5-5 reached 62.57% and 48.12%, respectively — representing a respective increase of approximately 1.89-fold and 1.45-fold compared to that achieved by M13 (36.45%). The closer proximity between naringenin and Cmpd I in mutants such as M4186 and M5-5 (3.80 Å and 3.84 Å) not only confers high catalytic activity but also enhances transformation efficiency. The successful outcomes achieved with M5-5 and M4186 mutants have demonstrated that the "flying kite model," starting from Cmpd I, is both reasonable and highly practical for the rational design of P450BM3. Reducing the catalytic distance could be a promising strategy for improving hydroxylation activity of P450 towards other steroids in future research endeavors. Importantly, these mutants exhibited no generation of any other by-products, highlighting their superior potential for industrial applications compared to other P450s. Furthermore, whole-cell catalysis products displayed prolonged survival time and increased stability within pomelo peels compared to enzyme alone, thereby enhancing the value of grapefruit processing.

Discussion

The steroids, alkanes, and flavonoids are widely present in plants waste, and further treatment of these wastes can improve the added value of products, and effectively avoid the damage to the environment (Acevedo-Rocha et al. 2018; Khan et al. 2021; Kille and Reetz 2011; Li and Reetz 2020; Sharma et al. 2017). Enzyme treatment was prevalent in agriculture processing for their wild catalytic condition (Amor and Ghoul 2010; Kaltenbach and Schröder 1999). However, most enzymes exhibit a limited substrate range. Overcoming this challenge in biochemistry involves expanding their substrate recognition capabilities as well as enhancing their catalytic efficiency towards non-natural complex

compounds (Chu and Sohng 2016; Hyster and Arnold 2015). The P450s have been extensively modified in biochemistry due to their spacious binding pocket and significant potential in medicinal biosynthesis (Kubo et al. 2006; Singh et al. 2015). However, the lack of a clear starting point for rational design has led to ongoing debates regarding strategies for modifying P450BM3, thereby impeding the efficiency of rational design.

In this study, we used Cmpd I as an initial starting point, assuming that a crucial aspect of P450BM3 rational design is to accurately induce ligand stretching manners and reduce the distance between C3′/C5′ and the O atom of Cmpd I. Thus, the "flying kite model" was proposed for the biocatalysis of naringenin. By applying the substrate correctly stretching in the binding pocket, we gradually reduced the catalytic distance between C3′ and Cmpd I, and obtained M4186 and M5-5 mutants based on M13 and inactivated P450BM3, respectively. The activity of M4186 was 4.27 times higher than that of M13, and the conversion rate of naringenin was 62.57%. These improved catalytic properties made the M4186 more suitable for the waste processing. The activity of M5-5 achieved through the same strategy was 1.48 times higher than that of M13, resulting in a conversion rate of naringenin at 48.12%, which significantly improved the synthesis efficiency of eriodictyol production. As shown in Fig. 3, the mutants of M4186 and M5-5 exhibited almost the same ligand binding manners. In the parallel conformation, the L437 forms ππ bonds with the B and A ring. In the vertical configuration, the S332 of M4186 forming an additional hydrogen bond with the carbonyl group on the substrate's C ring (Fig. 3). Furthermore, although E143G mutations do not directly participate in ligand binding, they can induce significant polarity and steric changes that may impact the active site size, thereby enhancing substrate affinity towards active Cmpd I (Fig. 4). The consistency of the docking mechanism and experimental data suggests that although the P450 enzyme captures the ligand into its active site through the flexibility of the F/G and B/C loops (Sevrioukova et al. 1999; Tripathi et al. 2013), the relative rigidity and stability of the active site facilitate consistent ligand binding, as observed in our docking simulations, which is a crucial factor contributing to the efficacy of our rational design strategy.

Considering that H· abstraction from substrate by Cpmd I is a crucial catalytic step (Luthra et al. 2011; Mak and Denisov 2018), closer proximity between Cmpd I's oxygen atom and naringenin's C3′ carbon would increase the likelihood of mutants exhibiting activity. Based on this mechanism, we propose a "flying kite model" which theoretically applies to non-natural substrates. By gradually positioning the ligand closer to CmpdI's catalytic center, hydroxylation mutants capable of producing naringenin can be obtained. The successful generation of M5-5 validates the rationale behind this design strategy. Considering the structure of naringenin with M5-5, M4186, and M13, the catalytic distance of the Cmpd I and the catalytic C atom of the naringenin was suggested to below 3.85 Å. This one-stop modification strategy provides a solid theoretical and practical example for developing P450s for non-substrate compounds. By employing the same model, mutants exhibiting activity towards steroids, alkanes, and flavonoids commonly found in agricultural waste can be feasibly generated, thereby enhancing the additional values of agricultural products.

Supplementary Information The online version contains supplementary material available at https://doi.org/10.1007/s00253-023-12867-9.

Author contribution XZ worked on the design of the protocol, experiments, and data analysis. YP helped with the experiments. YF worked on the writing and the visualization. YH and CZ assisted the writing and visualization. BF and JZ helped to design of the protocol. XL helped the computational calculation. BG and LL helped the visualization. HN provided the funding and guide the protocol. LZ provided of the funding, guide the protocol, data, and visualization.

Funding This work was supported by the National Key R&D Program of China (grant no. 2021YFC2102400), National Natural Science Foundation of China (grant nos. U1805235, 22208106), and Natural Science Foundation of Shanghai (grant nos. 21ZR1416500).

Data availability The data that support the findings of this study are available from the corresponding author upon reasonable request.

Declarations

Ethics declarations This article does not contain any studies with human participants or animals performed by any of the authors.

Conflict of interest The authors declare no competing interests.

References

Acevedo-Rocha CG, Gamble CG, Lonsdale R, Li A, Nett N, Hoebenreich S, Lingnau JB, Wirtz C, Fares C, Hinrichs H, Deege A, Mulholland AJ, Nov Y, Leys D, McLean KJ, Munro AW, Reetz MT (2018) P450-catalyzed regio- and diastereoselective steroid hydroxylation: efficient directed evolution enabled by mutability landscaping. ACS Catal 8(4):3395–3410. https://doi.org/10.1021/acscatal.8b00389

Amor IL, Ghoul M (2010) Biotransformation of naringenin to eriodictyol by Saccharomyces cerevisiea functionally expressing flavonoid 3' hydroxylase. Nat Prod Commun 5(12):1893–1898

Chen J, Cong Z (2019) Peroxide-driven hydroxylation of small alkanes catalyzed by an artificial P450BM3 peroxygenase system. ACS Catal 9(8):7350–7355. https://doi.org/10.1021/acscatal.9b02507

Chen W, Wong LL (2020) Oxidative diversification of steroids by nature-inspired scanning gycine mutagenesis of P450BM3 (CYP102A1). ACS Catal 10(15):8334–8343. https://doi.org/10.1021/acscatal.0c02077

Chu LL, Sohng JK (2016) Hydroxylation of diverse flavonoids by CYP450 BM3 variants: biosynthesis of eriodictyol from naringenin in whole cells and its biological activities. Microb Cell Fact 15(1):135. https://doi.org/10.1186/s12934-016-0533-4

Hong L-L, Kong J-Q (2020) Altering the regioselectivity of cytochrome P450 BM3 variant M13 toward Genistein through protein engineering and variation of reaction conditions. ACS Omega 5(49):32059–32066. https://doi.org/10.1021/acsomega.0c05088

Huang X, Groves JT (2017) Beyond ferryl-mediated hydroxylation: 40 years of the rebound mechanism and C-H activation. J Biol Inorg Chem: JBIC: Publ Soc Biol Inorg Chem 22(2–3):185–207. https://doi.org/10.1007/s00775-016-1414-3

Hyster TK, Arnold FH (2015) P450BM3-axial mutations: a gateway to non-natural reactivity. Isr J Chem 55(1):14–20. https://doi.org/10.1002/ijch.201400080

Jiang Y, Li S (2021) Unexpected reactions of α, β-unsaturated fatty acids provide insight into the mechanisms of CYP152 peroxygenases. Angew Chem Int Ed Engl 60(46):24694–24701. https://doi.org/10.1002/anie.202111163

Kaltenbach M, Schröder J (1999) Flavonoid hydroxylase from Catharanthus roseus: cDNA, heterologous expression, enzyme properties and cell-type specific expression in plants. Plant J 19(2):183–193. https://doi.org/10.1046/j.1365-313x.1999.00524.x

Karasawa M, Watanabe Y (2018) Whole-cell biotransformation of benzene to phenol catalysed by intracellular cytochrome P450BM3 activated by external additives. Angew Chem Int Ed Engl 57(38):12264–12269. https://doi.org/10.1002/anie.201804924

Kasai N, Sakaki T (2009) Enzymatic properties of cytochrome P450 catalyzing 3′-hydroxylation of naringenin from the white-rot fungus Phanerochaete chrysosporium. Biochem Biophys Res Commun 387(1):103–108. https://doi.org/10.1016/j.bbrc.2009.06.134

Khan UM, Sameen A, Aadil RM, Shahid M, Sezen S, Zarrabi A, Ozdemir B, Sevindik M, Kaplan DN, Selamoglu Z, Ydyrys A, Anitha T, Kumar M, Sharifi-Rad J, Butnariu M (2021) Citrus genus and its waste utilization: a review on health-promoting activities and industrial application. Evid Based Complement Alternat Med 2021:2488804. https://doi.org/10.1155/2021/2488804

Kille S, Reetz MT (2011) Regio- and stereoselectivity of P450-catalysed hydroxylation of steroids controlled by laboratory evolution. Nat Chem 3(9):738–743. https://doi.org/10.1038/nchem.1113

Kubo T, Peters MW, Meinhold P, Arnold FH (2006) Enantioselective epoxidation of terminal alkenes to (R)- and (S)-epoxides by engineered cytochromes P450 BM-3. Chemistry 12(4):1216–1220. https://doi.org/10.1002/chem.200500584

Lee ER, Cho SG (2007) The anti-apoptotic and anti-oxidant effect of eriodictyol on UV-induced apoptosis in keratinocytes. Biol Pharm Bull 30(1):32–37. https://doi.org/10.1248/bpb.30.32

Lee E, Kim Y (2013) Binding model for eriodictyol to Jun-N terminal kinase and its anti-inflammatory signaling pathway. BMB Rep 46(12):594–599. https://doi.org/10.5483/bmbrep.2013.46.12.092

Li A, Reetz MT (2020) Regio- and stereoselective steroid hydroxylation at C7 by cytochrome P450 monooxygenase mutants. Angew Chem Int Ed Engl 59(30):12499–12505. https://doi.org/10.1002/anie.202003139

Liu Y, Cong Y, Zhang C, Fang B, Pan Y, Li Q, You C, Gao B, Zhang JZH, Zhu T, Zhang L (2021) Engineering the biomimetic cofactors of NMNH for cytochrome P450 BM3 based on binding conformation refinement. RSC Adv 11(20):12036–12042. https://doi.org/10.1039/d1ra00352f

Luthra A, Denisov IG, Sligar SG (2011) Spectroscopic features of cytochrome P450 reaction intermediates. Arch Biochem Biophys 507(1):26–35. https://doi.org/10.1016/j.abb.2010.12.008

Lv Y, Zhou J (2019) Engineering enzymatic cascades for the efficient biotransformation of eugenol and taxifolin to silybin and isosilybin. Green Chem 21(7):1660–1667. https://doi.org/10.1039/C8GC03728K

Mak PJ, Denisov IG (2018) Spectroscopic studies of the cytochrome P450 reaction mechanisms. Biochim Biophys Acta Proteins Proteom 1:178–204. https://doi.org/10.1016/j.bbapap.2017.06.021

Nguyen NA, Yun C-H (2020a) Biocatalytic production of a potent inhibitor of adipocyte differentiation from phloretin using engineered CYP102A1. J Agric Food Chem 68(24):6683–6691. https://doi.org/10.1021/acs.jafc.0c03156

Nguyen THH, Yun C-H (2020b) Regioselective hydroxylation of naringin dihydrochalcone to produce neoeriocitrin dihydrochalcone by CYP102A1 (BM3) mutants. Catalysts 10(8):823

Nguyen NA, Yun C-H (2021) Enzymatic production of 3-OH phlorizin, a possible bioactive polyphenol from apples, by Bacillus megaterium CYP102A1 via regioselective hydroxylation. Antioxidants (Basel, Switzerland) 10(8):1327. https://doi.org/10.3390/antiox10081327

Nguyen NA, Cao NT, Nguyen THH, Ji J-H, Cha GS, Kang H-S, Yun C-H (2021) Enzymatic production of 3-OH phlorizin, a possible bioactive polyphenol from apples, by Bacillus megaterium CYP102A1 via regioselective hydroxylation. Antioxidants (Basel, Switzerland) 10(8):1327. https://doi.org/10.3390/antiox10081327

Ogliaro F, Shaik S (2002) Searching for the second oxidant in the catalytic cycle of cytochrome P450: a theoretical investigation of the iron(III)-hydroperoxo species and its epoxidation pathways. J Am Chem Soc 124(11):2806–2817. https://doi.org/10.1021/ja0171963

Owens DK, Winkel BS (2008) Biochemical and genetic characterization of Arabidopsis flavanone 3beta-hydroxylase. Plant Physiol Biochem 46(10):833–843. https://doi.org/10.1016/j.plaphy.2008.06.004

Rittle J, Green Michael T (2010) Cytochrome P450 compound I: capture, characterization, and C-H bond activation kinetics. Science 330(6006):933–937. https://doi.org/10.1126/science.1193478

Sevrioukova IF, Li H, Zhang H, Peterson JA, Poulos TL (1999) Structure of a cytochrome P450-redox partner electron-transfer complex. Proc Natl Acad Sci U S A 96(5):1863–1868. https://doi.org/10.1073/pnas.96.5.1863

Sharma K, Lee YR (2017) Converting citrus wastes into value-added products: economic and environmently friendly approaches. Nutrition 34:29–46. https://doi.org/10.1016/j.nut.2016.09.006

Sharma K, Mahato N, Cho MH, Lee YR (2017) Converting citrus wastes into value-added products: economic and environmently friendly approaches. Nutrition 34:29–46. https://doi.org/10.1016/j.nut.2016.09.006

Singh R, Kolev JN, Sutera PA, Fasan R (2015) Enzymatic C(sp(3))-H amination: P450-catalyzed conversion of carbonazidates into oxazolidinones. ACS Catal 5(3):1685–1691. https://doi.org/10.1021/cs5018612

Sligar SG (2010) Chemistry. Glimpsing the critical intermediate in cytochrome P450 oxidations. Science 330(6006):924–5. https://doi.org/10.1126/science.1197881

Su H, Shaik S (2019) Quantum-mechanical/molecular-mechanical studies of CYP11A1-catalyzed biosynthesis of pregnenolone from cholesterol reveal a C-C bond cleavage reaction that occurs by a compound I-mediated electron transfer. J Am Chem Soc 141(51):20079–20088. https://doi.org/10.1021/jacs.9b08561

Sun W, Li C (2020) Controlling chemo- and regioselectivity of a plant P450 in yeast cell toward rare licorice triterpenoid biosynthesis. ACS Catal 10:4253–4260

Tripathi S, Li H, Poulos TL (2013) Structural basis for effector control and redox partner recognition in cytochrome P450. Science 340(6137):1227–1230. https://doi.org/10.1126/science.1235797

Wang B, Shaik S (2015) Quantum mechanical/molecular mechanical calculated reactivity networks reveal how cytochrome P450cam and Its T252A mutant select their oxidation pathways. J Am Chem Soc 137(23):7379–7390. https://doi.org/10.1021/jacs.5b02800

Whitehouse CJ, Wong LL (2012) P450(BM3) (CYP102A1): connecting the dots. Chem Soc Rev 41(3):1218–1260. https://doi.org/10.1039/c1cs15192d